RSC Advances

PAPER

View Article Online
View Journal | View Issue

Cite this: *RSC Adv.*, 2019, **9**, 14982

One-pot synthesized Cu/Au/Pt trimetallic nanoparticles as a novel enzyme mimic for biosensing applications†

Pian Wu,[a] Ping Ding,[a] Xiaosheng Ye,*[ab] Lei Li,[c] Xiaoxiao He[b] and Kemin Wang[b]

Received 23rd January 2019
Accepted 4th May 2019

DOI: 10.1039/c9ra00603f

rsc.li/rsc-advances

Multimetallic nanomaterials have aroused special attention owing to the unique characteristics of chemical, optical and enhanced enzyme mimetic capabilities resulting from the synergistic effect of different metal elements. In this work, we present a facile, gentle, fast and one-pot method for preparing Cu/Au/Pt trimetallic nanoparticles (TNPs), which possess intrinsic and enhanced peroxidase-like activity as well as excellent stability, sustainable catalytic activity, and robustness to harsh environments. Kinetic analysis indicated that Cu/Au/Pt TNPs exhibited strong affinities with H_2O_2 and 3,3,5,5-tetramethylbenzidine (TMB) as the substrates. To investigate the feasibility of Cu/Au/Pt TNPs-based strategy in biological analysis, H_2O_2 was chosen as a model analyte and a sensitive and specific detection for H_2O_2 was acquired with a detection limit of 17 nM. By coupling with glucose oxidase (GOD), this assay could also achieve a sensitive and selective detection of glucose with a detection limit of 33 μM, indicating the versatility of the method. In view of the potential combination with diverse enzyme-related reactions, the Cu/Au/Pt TNPs-based strategy is promising as a universal platform for biosensors.

1. Introduction

Enzyme-based analytical strategies have aroused special attention due to advantages of low cost, easy operation, quick feedback, and no need of any advanced instrumentation. Artificial enzymes[1] are arousing great interest because of their excellent catalytic activity, high stability and low-cost compared with natural enzymes which can bear some serious disadvantages such as the catalytic activity being easily inhibited,[2] time-consuming and expensive process of preparation, purification and storage.[3] Over the past two decades, nanoparticle-based enzyme mimics, have seen tremendous progress as a result of the unique characteristics of nanomaterials such as large surface-to-volume ratio, superior optical and physical properties.[4] To date, many different types of enzyme mimics have been reported to catalyze a broad range of reactions for sensors, immunoassays and biomedical applications.[4,5]

Peroxidase enzymes, activating H_2O_2 to fulfil a large number of oxidation reactions in nature, have been widely applied in the fields of clinical and bioanalytical chemistry, where it is usually introduced for signaling or imaging by conjugating to an antibody as colorimetric substrates for enzymatic catalysis. Recently, numerous nanomaterials have been found to possess unexpected peroxidase-like activity. Yan and co-workers have discovered that ferromagnetic nanoparticles actually display a particular peroxidase-like activity.[6] And the detection of H_2O_2, glucose and thrombin was successfully achieved using Fe_3O_4 magnetic nanoparticles as peroxidase mimics.[7,8] Since the innovative work was reported by Yan *et al.*,[6] a great many of significant research focus have been placed on developing various nanomaterials with peroxidase activity and being in search of the potential applications. For instance, graphene oxide nanoparticles,[9] iridium nanoparticles,[10] Co_3O_4 nanoparticles,[11] $CoFe_2O_4$ magnetic nanoparticles,[12] V_2O_5 nanoparticles,[13] Au@PO–CeO_2 NPs,[14] dopamine coated Fe_3O_4,[15] CuS concave superstructures,[16] and CeO_{2-x} NPs[17] were also found with oxidase- or peroxidase-like activity. The new discoveries and functions make them potentially useful in the fields of sensor and environmental chemistry. However, there are still some deficiencies needed to be improved for further biosensing or biomedical applications, such as insufficient catalytic activity, harsh synthesis and purification process, poor biocompatibility, difficulty to be modified, and so on.

Multicomponent metal nanoparticle is a kind of novel materials with different functionalities through incorporating three or more different elements to the alloy, which usually

[a]XiangYa School of Public Health, Central South University, Changsha 410078, Hunan, China. E-mail: yexiaosheng@csu.edu.cn; Fax: +86-731-84805462; Tel: +86-731-84805462

[b]State Key Laboratory of Chemo/Biosensing and Chemometrics, College of Chemistry and Chemical Engineering, Institute of Biology, Hunan University, Key Laboratory for Bio-Nanotechnology and Molecular Engineering of Hunan Province, Changsha 410082, Hunan, China

[c]Center for Global Health, School of Public Health, Nanjing Medical University, Nanjing 211166, Jiangsu, China

† Electronic supplementary information (ESI) available. See DOI: 10.1039/c9ra00603f

provide novel or enhanced properties owing to various synergistic effects in comparison to monometallic or bimetallic nanoparticles.[18,19] Key properties of multimetallic nanomaterials such as optical and catalytic properties could be modified or improved by controlling their morphologies, structures and chemical compositions, thus leading to catalyst, sensor and medical applications.[20,21] At present, there are several popular elements in the field of multimetallic nanomaterials, including platinum (Pt), gold (Au), and copper (Cu). As an element with unique catalytic feature, Pt has been widely used for important catalysis[22] and electrocatalysis applications.[23,24] However, considering the limited resource, difficulty to be modified and rising cost of Pt, it is urgent to find the substitute for pure Pt catalysts. As a particular species of great service, Au nanomaterials possess unique properties such as biocompatibility, flexible modification[25] and catalytic effect towards many important oxidization reactions, which make them excellent scaffolds for the fabrication of novel sensors and catalytic analysis.[26,27] Moreover, as another coinage metal, Cu-based semiconductor nanomaterials have been widely explored with the properties of well defined shapes[28,29] and enhanced catalytic performance for Pt nanoparticles.[30] Thus, we envisage that the combination of Pt with Cu and Au will probably be a good method to make up the drawbacks of pure Pt nanomaterials as well as achieve the fusion of different functionalities such as good compatibility, facile modification[31] and enhanced or multiple enzyme mimetic capabilities.[32]

Herein, a fast, gentle and one-pot synthetic method was utilized to fabricate Cu/Au/Pt TNPs with enhanced catalytic performance. As a novel enzyme mimic with peroxidase-like activity, Cu/Au/Pt TNPs could catalyze the oxidation of the peroxidase substrate TMB by H_2O_2 to develop a blue color in aqueous solution. This provided a sensitive colorimetric detection of H_2O_2 which is of critical importance in the application fields of organic synthesis, food production, paper bleaching, pharmaceutical, clinical and environmental analysis[33] as well as in many biological processes like cell signaling.[34] By coupling the catalytic oxidation reaction of glucose by GOD, the colorimetric strategy was further applied for quantitative detection of glucose. The strategy showed great potentials as a universal tool for biosensing in view of the potential combination with diverse enzyme-related reactions.[35]

2. Experimental

2.1. Chemicals and reagents

Horseradish peroxidase (HRP, 50–150 units per mg), glucose oxidase (GOD, from *Aspergillus niger*), 30% H_2O_2 and K_2PtCl_4 (>99.9%) were obtained from Sigma-Aldrich Chemicals (St. Louis, USA). $HAuCl_4 \cdot H_2O$ (>99.5%), $CuSO_4 \cdot 5H_2O$, 3,3,5,5-tetramethylbenzidine (TMB), $NaBH_4$, sodium citrate, NaClO and $NaNO_2$ were purchased from Ding Guo Biotech Co., Ltd. (Beijing, China). Glucose, *R*-lactose, D-fructose and maltose were obtained from Aladdin Industrial Inc. (Shanghai, China). All other reagents were of the highest grade available. Deionized water was obtained through the Nanopure Infinity™ ultrapure water system (Barnstead/Thermolyne Corp.).

2.2. Synthesis and characterization of Cu/Au/Pt TNPs

Generally, 12 μL of 0.1 M $CuSO_4$ and 25 μL of 0.1 M sodium citrate were added into 10 mL of water. Afterward, 0.5 mL of freshly prepared $NaBH_4$ (25 mM) was rapidly injected into the mixture above. About 15 min later, the mixed solution was added with the mixture of 25 μL $HAuCl_4$ (0.1 M) and 25 μL K_2PtCl_4 (0.1 M) and kept stirring for 20 min. The final Cu/Au/Pt TNPs solution was stored at room temperature before its further application. X-ray energy-dispersive spectroscopy (EDS) and high-resolution transmission electron microscopy (HRTEM) were performed on a JEOL-3010 microscope operating at an accelerating voltage of 200 kV. The elemental mapping of Cu/Au/Pt TNPs was analyzed on Titan G2 microscope at an accelerating voltage of 300 kV. All TEM samples were deposited on Mo supporting film and dried overnight before examination.

2.3. Study of Cu/Au/Pt TNPs catalytic performance

The catalytic activity of Cu/Au/Pt TNPs for TMB–H_2O_2 reaction was investigated using the following procedures: Cu/Au/Pt TNPs (7 μg mL^{-1}) were incubated with 250 μL of sodium acetate buffer (0.5 M, pH 4.0) solution containing 333 μM TMB (freshly prepared) and 10 μM H_2O_2. After the mixed solution was incubated in a 30 °C water bath for 10 min, photos were taken immediately, and the spectra or the absorbance of the oxidation product of TMB at 650 nm were recorded using an Infinite M1000 multifunctional micro-plate reader through adding 150 μL of the resulting solution into a 96-well plate. The catalytic activity of HRP was also determined by incubation with 20 ng mL^{-1} HRP, 333 μM TMB, and 10 μM H_2O_2.

To investigate the influence of incubation temperature on the relative activity of Cu/Au/Pt TNPs and HRP, catalytic reactions were performed at a range between 20–65 °C under the same conditions with the above used. To examine the influence of reaction buffer pH on the relative activity of Cu/Au/Pt TNPs and HRP, 0.5 M sodium acetate buffer solutions (pH 1.0–12.0) were utilized. To study the stability of peroxidase-like activity, Cu/Au/Pt TNPs and HRP were stored at room temperature, and the catalytic activity was determined every 24 hours for consecutive 7 days.

2.4. Kinetic analysis

Kinetic assays were carried out by recording the absorbance at 650 nm in every minute. A series of initial reaction rates with varying concentration of TMB and a fixed concentration of H_2O_2 or *vice versa* were obtained to investigate the kinetic characteristics. In this experiment, the concentrations of H_2O_2 and TMB were fixed at 1.6 mM and 0.2 mM, respectively. The apparent kinetic parameters were calculated in the light of Lineweaver–Burk plots based on the Michaelis–Menten eqn (1):

$$1/v = K_m/V_m(1/[S]+1/K_m) \quad (1)$$

where v is the initial velocity, V_{max} is the maximal reaction velocity, [S] is the concentration of substrate (TMB or H_2O_2), K_m is the Michaelis constant.

2.5. H_2O_2 sensing

50 μL of Cu/Au/Pt TNPs (350 μg mL^{-1}), 7.5 μL of TMB (16.6 mM), and 10 μL of H_2O_2 with various concentrations were mixed with 182.5 μL of sodium acetate buffer (0.5 M, pH 5.0) solution, incubated in a 55 °C water bath for 10 min. Subsequently, photos were taken immediately, and the spectra or the absorbance at 650 nm were recorded using an Infinite M1000 multifunctional micro-plate reader through adding 150 μL of the resulting solution into a 96-well plate.

2.6. Glucose sensing

Glucose detection was performed as follows: 45 μL of glucose with different concentrations in 10 mM phosphate buffer solution (pH 7.0) was mixed with 5 μL of 5.0 mg mL^{-1} GOD and incubated at a 37 °C water bath for 15 min. Then, 50 μL of Cu/Au/Pt TNPs (350 μg mL^{-1}), 5 μL of TMB (16.6 mM), and 145 μL of sodium acetate buffer (0.5 M, pH 5.0) solution were added to the above 50 μL of reaction solution. After incubation in a 55 °C water bath for 10 min, the absorbance of the oxidation product of TMB at 650 nm was recorded using an Infinite M1000 multifunctional micro-plate reader through adding 150 μL of the resulting solution into a 96-well plate. The capability of detection in complex samples was also analyzed by using fetal bovine serum as the model. Glucose was analyzed in PBS solution (pH 7.0) containing 4% of serum in volume.

3. Results and discussions

3.1. Synthesis and characterization of Cu/Au/Pt TNPs

Cu/Au/Pt TNPs were synthesized using a facile one-pot protocol through the co-reduction of $CuSO_4$, $HAuCl_4$ and K_2PtCl_4 in the presence of $NaBH_4$ at room temperature. Subsequently, the size, morphology and element compositions of Cu/Au/Pt TNPs were systematically investigated. It was seen from the TEM image (Fig. 1A) that the as-prepared Cu/Au/Pt TNPs were earthworm-like with an average size of ~20 nm. Roughly uniform distribution of Cu, Au and Pt in the TNP was observed through element mapping analysis of single Cu/Au/Pt TNP (Fig. 1B–F), which was also confirmed by EDS spectrum (Fig. 1G).

To validate the peroxidase-like activity of Cu/Au/Pt TNPs, the catalysis of a popular substrate TMB in peroxidase-based detection systems was studied in the presence of H_2O_2. As seen from Fig. 2A, it was found that TMB added with Cu/Au/Pt TNPs and H_2O_2 exhibited obvious adsorption peak at around 650 nm originating from the oxidation of TMB,[36,37] while TMB in the absence of Cu/Au/Pt TNPs or H_2O_2 showed no appearance of the oxidation peak ranging from 500 to 800 nm. The inset of Fig. 2A showed the color change of the corresponding samples, and the result was in accord with the spectra variation mentioned above evidencing that the nanomaterials could catalyze the oxidation of TMB. And it was shown in Fig. 2B that the catalytic activity of Cu/Au/Pt TNPs was obviously enhanced in comparison with monometallic or bimetallic nanoparticles under the same conditions, which mainly attributed to the synergistic effect of three metal elements. Then, the effects of the contents of three metal elements on the properties of Cu/Au/Pt TNPs were also investigated (Fig. S1†), it could be found that the contents of Cu, Au, and Pt elements had little influence on the peroxidase-like activity of Cu/Au/Pt TNPs. All these results confirmed that the Cu/Au/Pt TNPs displayed an intrinsic enhanced peroxidase-like activity.

3.2. Study of Cu/Au/Pt TNPs catalytic performance

It is well-known that the catalytic ability of enzyme mimics or natural enzyme is affected by environment aspects.[1] Thus it is very important to study the effects of experimental conditions on Cu/Au/Pt TNPs to gain an optimal catalytic activity. For comparison, HRP-based method was also studied. As shown in Fig. 3A, Cu/Au/Pt TNPs preserved a high catalytic activity from 20 to 65 °C with a maximum value at 55 °C. The thermal stability of the nanoparticles catalytic activity can be promising for industrial applications at high temperatures. For comparison, the activity of HRP obviously dropped when the temperature surpassed 30 °C, though it maintained stable catalytic activity but 2–3 times lower than the initial activity. This suggested the

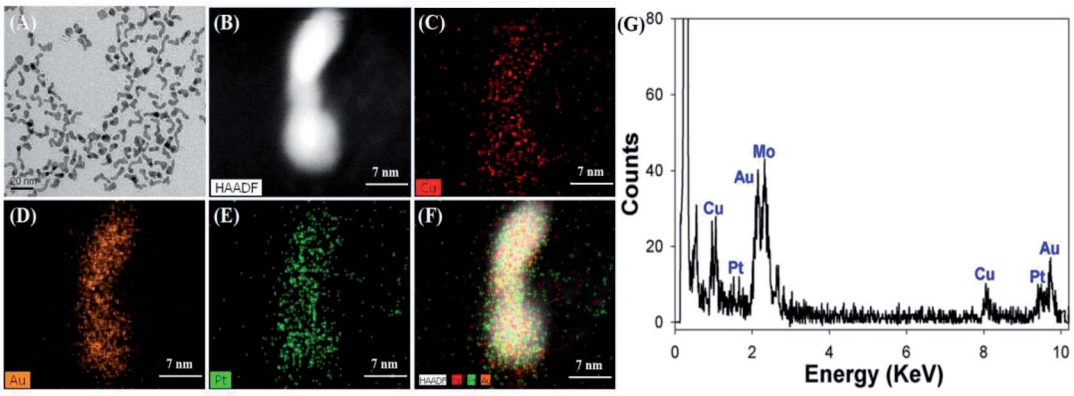

Fig. 1 Synthesis and characterization of Cu/Au/Pt TNPs. (A) TEM image of Cu/Au/Pt TNPs. (B) STEM image of an individual Cu/Au/Pt TNP. (C–E) STEM-EDX elemental mapping image of (C) Cu, (D) Au and (E) Pt of an individual Cu/Au/Pt TNP. (F) The merged image of C, D and E. (G) EDS result of Cu/Au/Pt TNPs.

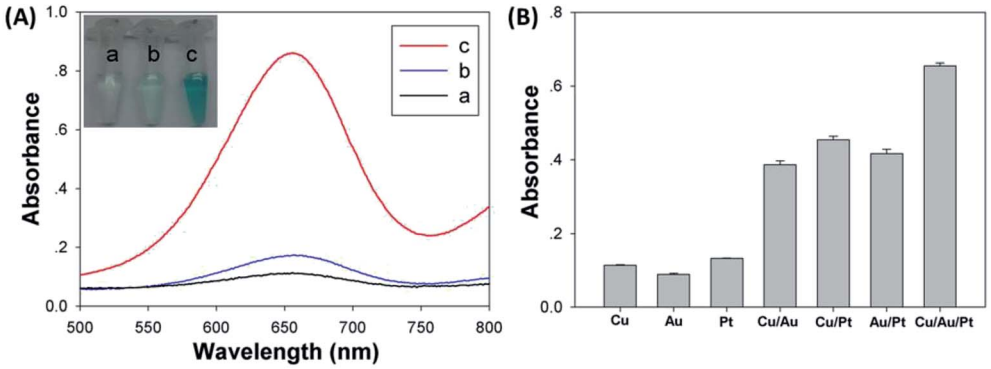

Fig. 2 (A) Typical absorption spectra of TMB–H_2O_2 mixed solution in the absence and presence of Cu/Au/Pt TNPs: (a) TMB + Cu/Au/Pt TNPs, (b) TMB + H_2O_2, (c) TMB + H_2O_2 + Cu/Au/Pt TNPs. Inset shows the photograph of the solutions. (B) Catalytic activity of Cu/Au/Pt TNPs for TMB–H_2O_2 reaction compared with other kinds of nanoparticles prepared with different chemicals added in the same reaction system.

catalytic activity of Cu/Au/Pt TNPs was less susceptible to temperature changes than HPR. At this temperature, we also investigated the catalytic activity of Cu/Au/Pt TNPs and HRP at various pH, respectively. As shown in Fig. 3B, the catalytic activity of Cu/Au/Pt TNPs and HRP both increased with the rising pH from 3.0 to 7.0, and then decreased. The optimal pH values of two methods were both 5.0. Accordingly, all of the results evidenced that the catalytic activity of Cu/Au/Pt TNPs kept stable between wide temperature changes under certain pH ranges comparing with HRP.

Furthermore, it is very essential to test the storage stability of nanozyme, which is an important factor to be considered in practical applications. Therefore, in order to study the ability of Cu/Au/Pt TNPs to maintain the activity over a long period of time, the same batch of Cu/Au/Pt TNPs was determined based on the same analytical treatment over 7 days. HRP, stored at room temperature when not in use, was used as control enzyme. As indicated from Fig. 3C, the peroxidase-like activity of Cu/Au/Pt TNPs remained excellent without damage over 7 days, showing excellent stability. In contrast, the activity of HRP decreased obviously a day later, which is in accordance with the fact that HRP has low stability and is easy to be inactive in circumjacent environments. Thus, Cu/Au/Pt TNPs, as peroxidase mimics, exhibited insensitivity to surrounding conditions and could maintain high catalytic activity over a long period of time. Compared with HRP, Cu/Au/Pt TNPs show several merits, such as increased stability, sustainable catalytic property, and robustness to rigorous environments. These will promote the analytical and biomedical applications of Cu/Au/Pt TNPs in view of the modification of targeting molecules on the surface of nanoparticles by "Au–S" interaction.[25,31]

3.3. Kinetic analysis

The catalytic activities of Cu/Au/Pt TNPs were studied by steady-state kinetics. The typical Michaelis–Menten curves could be acquired with the concentration of one substrate fixed and the other varied (Fig. 4A and B), and the enzyme kinetic parameters of hyperbola were shown in Table 1. K_m was considered as a specific reflection of enzyme affinity to substrates and a low K_m value indicated a strong affinity.[38] The results in Table 1 indicated that the K_m value of Cu/Au/Pt TNPs with both H_2O_2 and TMB is much lower compared to natural enzyme HRP and other reported nanomaterials with peroxidase-like activities, suggesting that Cu/Au/Pt TNPs have a much higher affinity for two substrates.

3.4. H_2O_2 sensing

Development of novel biosensors is crucial in the fields of food production, environmental analysis, diseases diagnostics and so on. H_2O_2 was chosen as a model analyte due to its critical applications in organic synthesis, paper bleaching, pharmaceutical and many biological processes.[33,34] Utilizing the catalysis of Cu/Au/Pt TNPs upon TMB–H_2O_2 reaction and the dependence of colorimetric signal output on the concentration of H_2O_2 to construct a Cu/Au/Pt TNPs-based biosensing platform. The concentration dependence of H_2O_2 was firstly evaluated by the TMB–H_2O_2 reaction in the presence of Cu/Au/Pt TNPs, it was shown in Fig. S2† that the absorbances at 650 nm were different under various H_2O_2 concentrations and increased with the increasing of reaction time except in the absence of H_2O_2, which were attributed to the charge-transfer complexes derived from the one-electron oxidation of TMB. To achieve an optimized detection, optimization of Cu/Au/Pt TNPs concentrations and response time towards H_2O_2 concentrations were first conducted, revealing a signal plateaus achieved when the Cu/Au/Pt TNPs concentration was 0.07 mg mL^{-1} and the response time was 10 min (Fig. S3†). Thus, on the basis of the conditions optimization described above, colorimetric detection of H_2O_2 was conducted in sodium acetate buffer (pH 5.0) at 55 °C with a nanoparticle concentration of 0.07 mg mL^{-1} and reaction time of 10 min. It was found from Fig. 5A that the solution color changed from light blue to dark blue as the concentration of H_2O_2 increased and a concentration of 50 nM H_2O_2 could even be distinguished by the naked eye. The corresponding absorbance spectra change was also recorded presenting in Fig. 5B, in agreement with the result of Fig. 5A. Subsequently, the absorbance at 650 nm was collected for quantitative detection of H_2O_2. As shown in Fig. 5C, it was revealed that the absorbance intensity at 650 nm rose with increasing H_2O_2 concentration from 0.05 to 10 μM, implying

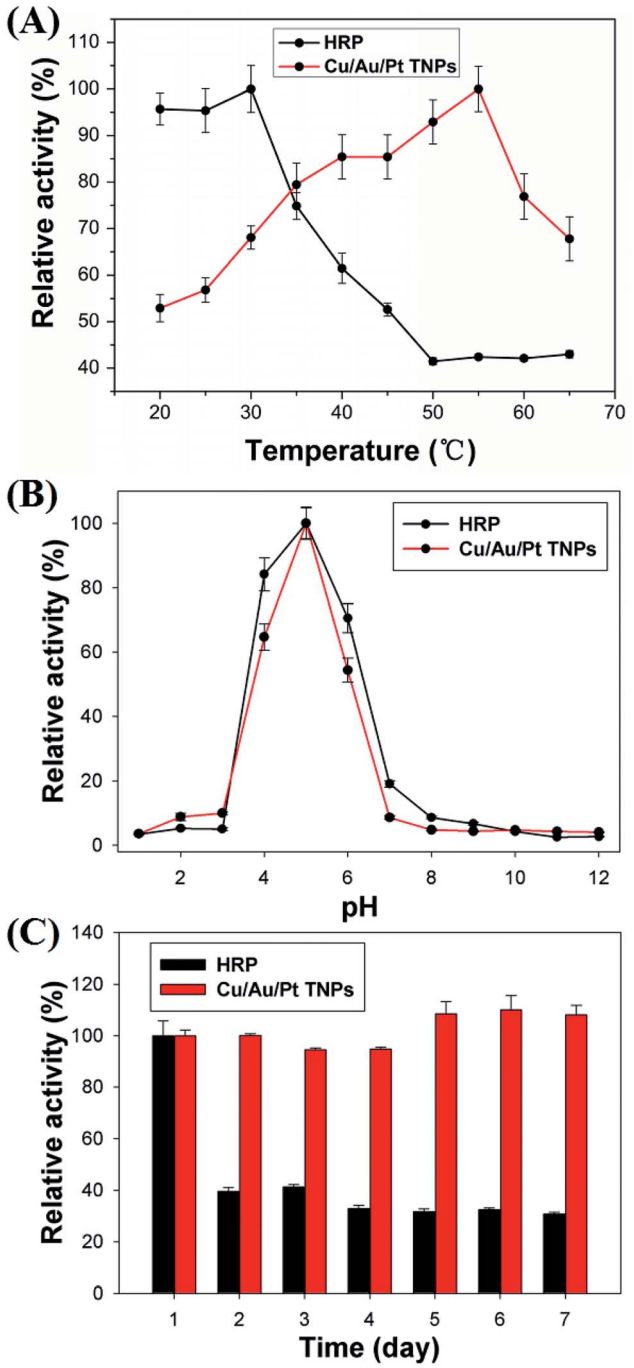

Fig. 3 Stability comparison between Cu/Au/Pt TNPs and HRP. Peroxidase activities of Cu/Au/Pt TNPs and HRP were measured at (A) 20–65 °C or (B) pH 1–12 under standard conditions. (C) Long-term stability of Cu/Au/Pt TNPs and HRP stored at room temperature. The maximum point in each curve (A–C) was set as 100%. The maximum point in each curve (A–C) was set as 100%.

a relatively broad response range based on this catalytic reaction system. There was a good linear correlation between the absorbance intensity and H_2O_2 concentration in the range of 0–1000 nM ($R^2 = 0.9921$), with a detection limit of 17 nM (LOD is equal to 3 times standard deviation of the blank sample divided by slope of the analytical calibration), which provided a lower

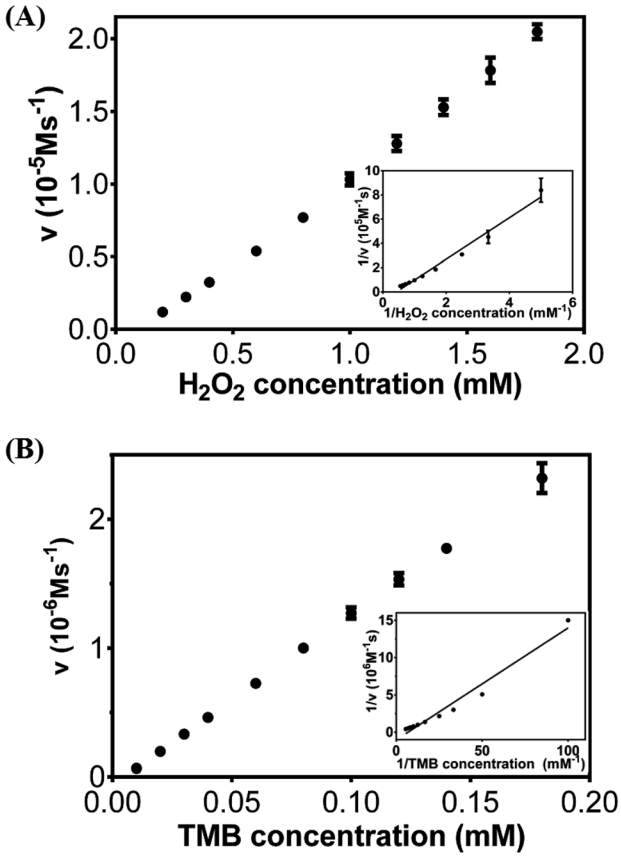

Fig. 4 Steady-state kinetic assay by the Michaelis–Menten model and Lineweaver–Burk model for (A) Cu/Au/Pt TNPs with 0.2 mM TMB and varied concentration of H_2O_2. (B) Cu/Au/Pt TNPs with 1.6 mM H_2O_2 and varied concentration of TMB.

detection limit than the previous reported colorimetric method (Table S1†). In addition, Cu/Au/Pt TNPs exhibited good specificity to H_2O_2 (Fig. S4†).

3.5. Glucose sensing

To verify the versatility of the Cu/Au/Pt TNPs-based biosensing platform, a quantitative analysis of glucose was further

Table 1 The comparison of Cu/Au/Pt TNPs with other reported enzyme mimics and HRP in kinetic parameters

Enzyme mimics	Substrate	K_m (mM)	V_{max} (10^{-7} M s^{-1})	Ref.
Cu/Au/Pt TNPs	H_2O_2	2.34	136.5	This work
	TMB	0.15	7.33	
HRP	H_2O_2	3.70	0.87	7
	TMB	0.43	1.00	
Au NPs	H_2O_2	45.83	1.07	39
	TMB	0.74	1.22	
Fe_3O_4	H_2O_2	1175.30	0.24	40
	TMB	0.49	0.56	
Fe_3O_4@Pt	H_2O_2	702.6	7.14	40
	TMB	0.15	0.71	
GO–AuNCs	H_2O_2	142.39		38
	TMB	0.16		
Ft–Pt NPs	H_2O_2	187.25	3200	41
	TMB	0.22	5.58	

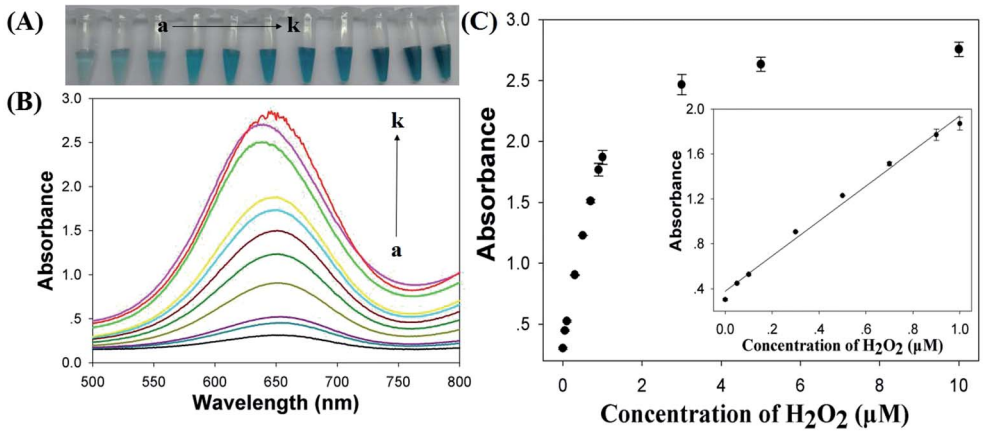

Fig. 5 Detection of H_2O_2 with different concentrations using Cu/Au/Pt TNPs-based biosensing strategy. (A) Photographs and (B) absorption spectra (from a to k: 0, 0.05, 0.1, 0.3, 0.5, 0.7, 0.9, 1, 3, 5, and 10 μM). (C) Dependence of the absorbance at 650 nm on the concentration of H_2O_2 in the range from 0 to 10 μM. Inset shows the corresponding linear calibration plots.

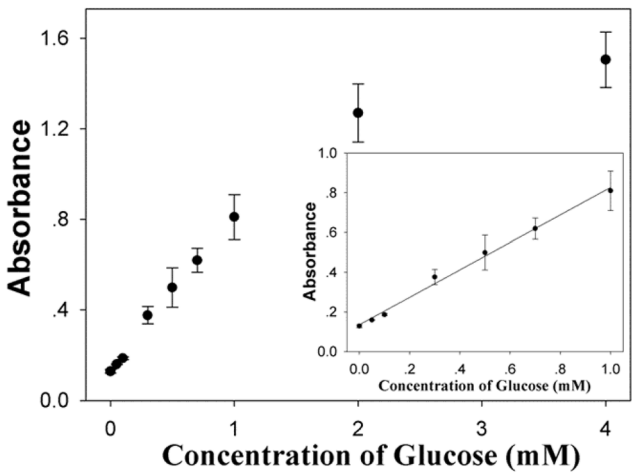

Fig. 6 Detection of glucose with different concentrations using Cu/Au/Pt TNPs-based biosensing strategy. Inset shows the corresponding linear calibration plots.

performed by combining the Cu/Au/Pt TNPs-catalyzed TMB–H_2O_2 system with the oxidation of glucose by GOD. Since the catalytic activity of GOD is not the best at pH 5.0 and 55 °C, glucose determination was carried out in two separated steps. Glucose and GOD were first reacted to produce gluconic acid and H_2O_2 in PBS (pH 7.0) at 37 °C for 15 min. Subsequently, the resulted H_2O_2 was detected using the TMB–Cu/Au/Pt TNPs reaction system at pH 5.0 and 55 °C. As seen from Fig. 6, the absorbance intensity (650 nm) increased with increasing glucose concentration from 0 to 4 mM with a detectable minimum concentration of 0.05 mM. There was a good linear response range between 0–1 mM (the inset of Fig. 6), with a detection limit of 33 μM. Because the glucose concentration of diabetes patients is at a level ≥7 mM,[42] the detection ability of this assay can meet the need for clinical application.

Selectivity is another major aspect to be considered in analysis. And we chose fructose, lactose and maltose as control samples. As shown in Fig. 7A, glucose displayed obvious absorbance at 650 nm while no detectable signals were obtained for other control samples even though the concentrations of samples were tenfold higher (5 mM) than that of glucose, indicating high selectivity of this strategy toward glucose detection. To further evaluate the feasibility of this method in real sample, a primary application was facilitated by using 4% of serum (fetal bovine serum) in volume to prepare samples. As

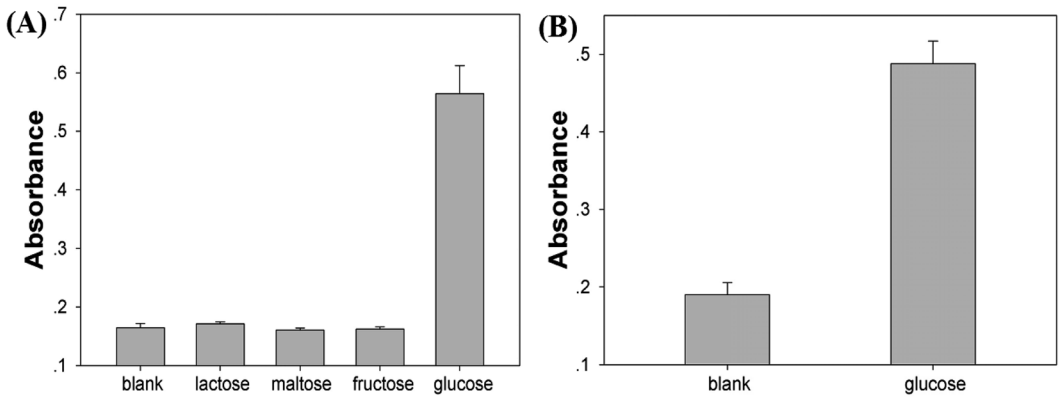

Fig. 7 (A) Determination of the selectivity of glucose detection with no saccharide, 5 mM lactose, 5 mM maltose, 5 mM fructose and 0.5 mM glucose. (B) Detection of glucose in diluted serum samples using Cu/Au/Pt TNPs as peroxidase mimic-based method.

shown in Fig. 7B, the absorption signals induced by glucose were much higher than blank group, implying that the Cu/Au/Pt TNPs-based analytical platform could satisfy the analysis of glucose in the blood samples of diabetic patients.

4. Conclusion

In conclusion, we reported a facile, gentle, fast and one-pot method for preparing Cu/Au/Pt TNPs based on the co-reduction of $CuSO_4$, $HAuCl_4$ and K_2PtCl_4 in the presence of $NaBH_4$. The results showed that Cu/Au/Pt TNPs possessed intrinsic peroxidase-like activity as well as increased stability, sustainable catalytic activity, and robustness to harsh environments. Kinetic analysis indicated that Cu/Au/Pt TNPs exhibited strong affinities with H_2O_2 and TMB as the substrates. Cu/Au/Pt TNPs as a peroxidase mimic provided a sensitive colorimetric assay for specific detection of H_2O_2 with a detection limit of 17 nM. By coupling with GOD, Cu/Au/Pt TNPs-based strategy could also achieve a selective and sensitive detection of glucose with a detection limit of 33 μM. In view of the potential combination with diverse enzyme-related reactions, Cu/Au/Pt TNPs as a novel enzyme mimic showed a great potential as a universal platform for applications in biosensors.[35]

Conflicts of interest

There are no conflict of interest to declare.

Acknowledgements

This work was supported by the Fundamental Research Funds for the Central Universities, and National Natural Science Foundation of China (Grant No. 21676305).

References

1 H. Wei and E. Wang, *Chem. Soc. Rev.*, 2013, **42**, 6060–6093.
2 E. Shoji and M. S. Freund, *J. Am. Chem. Soc.*, 2001, **123**, 3383–3384.
3 M. Nasir, M. H. Nawaz, U. Latif, M. Yaqub, A. Hayat and A. Rahim, *Microchim. Acta*, 2016, **184**, 1–20.
4 B. Liu and J. Liu, *Nano Res.*, 2017, **10**, 1125–1148.
5 F. Manea, F. B. Houillon, L. Pasquato and P. Scrimin, *Angew. Chem.*, 2004, **116**, 6291–6295.
6 L. Gao, J. Zhuang, L. Nie, J. Zhang, Y. Zhang, N. Gu, T. Wang, J. Feng, D. Yang, S. Perrett and X. Yan, *Nat. Nanotechnol.*, 2007, **2**, 577–583.
7 H. Wei and E. Wang, *Anal. Chem.*, 2008, **80**, 2250–2254.
8 Z. Zhang, Z. Wang, X. Wang and X. Yang, *Sens. Actuators, B*, 2010, **147**, 428–433.
9 S. Wang, R. Cazelles, W. C. Liao, M. Vázquez-González, A. Zoabi, R. Abu-Reziq and I. Willner, *Nano Lett.*, 2017, **17**, 2043–2048.
10 M. Cui, J. Zhou, Y. Zhao and Q. Song, *Sens. Actuators, B*, 2017, **243**, 203–210.
11 H. Jia, D. Yang, X. Han, J. Cai, H. Liu and W. He, *Nanoscale*, 2016, **8**, 5938–5945.
12 W. Shi, X. Zhang, S. He and Y. Huang, *Chem. Commun.*, 2011, **47**, 10785–10787.
13 R. André, F. Natálio, M. Humanes, J. Leppin, K. Heinze, R. Wever, H. C. Schröder, W. E. G. Müller and W. Tremel, *Adv. Funct. Mater.*, 2011, **21**, 501–509.
14 Q. Kong, K. Cui, L. Zhang, Y. Wang, J. Sun, S. Ge, Y. Zhang and J. Yu, *Anal. Chem.*, 2018, **90**, 11297–11304.
15 S. Mumtaz, L. Wang, S. Z. Hussain, M. Abdullah, Z. Huma, Z. Iqbal, B. Creran and V. M. R. I. Hussain, *Chem. Commun.*, 2017, **53**, 12306–12308.
16 W. He, H. Jia, X. Li, Y. Lei, J. Li, H. Zhao, L. Mi, L. Zhang and Z. Zheng, *Nanoscale*, 2012, **4**, 3501–3506.
17 V. Patel, M. Singh, E. L. H. Mayes, A. Martinez, V. Shutthanandan, V. Bansal, S. Singh and A. S. Karakoti, *Chem. Commun.*, 2018, **54**, 13973–13976.
18 J. Zhang, J. Ma, X. Fan, W. Peng, G. Zhang, F. Zhang and Y. Li, *Catal. Commun.*, 2017, **89**, 148–151.
19 X. Ye, J. Chen, B. T. Diroll and C. B. Murray, *Nano Lett.*, 2013, **13**, 1291–1297.
20 S. W. Kang, Y. W. Lee, Y. Park, B. S. Choi, J. W. Hong, K. H. Park and S. W. Han, *ACS Nano*, 2013, **7**, 7945–7955.
21 S. Ge, Y. Zhang, L. Zhang, L. Liang, H. Liu, M. Yan, J. Huang and J. Yu, *Sens. Actuators, B*, 2015, **220**, 665–672.
22 Y. Ju and J. Kim, *Chem. Commun.*, 2015, **51**, 13752–13755.
23 J. Liu, X. Bo, Z. Zhao and L. Guo, *Biosens. Bioelectron.*, 2015, **74**, 71–77.
24 S. Wu, J. Liu, Z. Tian, Y. Cai, Y. Ye, Q. Yuan and C. Liang, *ACS Appl. Mater. Interfaces*, 2015, **7**, 22935–22940.
25 X. Zhu, J. Zhao, Y. Wu, Z. Shen and G. Li, *Anal. Chem.*, 2011, **83**, 4085–4089.
26 J. Zheng, Y. Hu, J. Bai, C. Ma, J. Li, Y. Li, M. Shi, W. Tan and R. Yang, *Anal. Chem.*, 2014, **86**, 2205–2212.
27 F. Chen, Y. Zhao, C. Fan and Y. Zhao, *Anal. Chem.*, 2015, **87**, 8718–8723.
28 P. Lignier, R. Bellabarba and R. P. Tooze, *Chem. Soc. Rev.*, 2012, **41**, 1708–1720.
29 D. Zhang, R. Wang, M. Wen, D. Weng, X. Cui, J. Sun, H. Li and Y. Lu, *J. Am. Chem. Soc.*, 2012, **134**, 14283–14286.
30 X. Ge, L. Chen, J. Kang, T. Fujita, A. Hirata, W. Zhang, J. Jiang and M. Chen, *Adv. Funct. Mater.*, 2013, **23**, 4156–4162.
31 J. Li, B. Zhu, X. Yao, Y. Zhang, Z. Zhu, S. Tu, S. Jia, R. Liu, H. Kang and C. J. Yang, *ACS Appl. Mater. Interfaces*, 2014, **6**, 16800–16807.
32 W. He, Y. Liu, J. Yuan, J. Yin, X. Wu, X. Hu, K. Zhang, J. Liu, C. Chen, Y. Ji and Y. Guo, *Biomaterials*, 2011, **32**, 1139–1147.
33 D. Chirizzi, M. Rachele Guascito, E. Filippo, C. Malitesta and A. Tepore, *Talanta*, 2016, **147**, 124–131.
34 O. H. Petersen, A. Spät and A. Verkhratsky, *Philos. Trans. R. Soc., B*, 2005, **360**, 2197–2199.
35 H. Wang, X. Liu, C. H. Lu and I. Willner, *ACS Nano*, 2013, **7**, 7278–7286.
36 Y. Jv, B. Li and R. Cao, *Chem. Commun.*, 2010, **46**, 8017–8019.
37 C. Lu, X. Liu, Y. Li, F. Yu, L. Tang, Y. Hu and Y. Ying, *ACS Appl. Mater. Interfaces*, 2015, **7**, 15395–15402.

38 Y. Tao, Y. Lin, Z. Huang, J. Ren and X. Qu, *Adv. Mater.*, 2013, **25**, 2594–2599.
39 X. Chen, X. Tian, B. Su, Z. Huang, X. Che and M. Oyama, *Dalton Trans.*, 2014, **43**, 7449–7454.
40 M. Ma, J. Xie, Y. Zhang, Z. Chen and N. Gu, *Mater. Lett.*, 2013, **105**, 36–39.
41 J. Fan, J. J. Yin, B. Ning, X. Wu, Y. Hu, M. Ferrari, G. J. Anderson, J. Wei, Y. Zhao and G. Nie, *Biomaterials*, 2011, **32**, 1611–1618.
42 Y. Zhang, E. T. Lee, R. B. Devereux, J. Yeh, L. G. Best, R. R. Fabsitz and B. V. Howard, *Hypertension*, 2006, **47**, 410–414.